Supplementary Information for:

Chelation-Assisted Formation of Multi-Yolk-Shell Co_4N@Carbon Nanoboxes for Self-Discharge-Suppressed High-Performance Li-SeS_2 Batteries

Tao Chen,[a,†] Weihua Kong,[a,†] Mengting Fan,[a,†] Zewen Zhang,[a] Lei Wang,[a] Renpeng Chen,[a] Yi Hu,[a] Jing Ma,*[,a] and Zhong Jin*[,a,b]

[a]Key Laboratory of Mesoscopic Chemistry of MOE, Jiangsu Key Laboratory of Advanced Organic Materials, School of Chemistry and Chemical Engineering, Nanjing University, Nanjing 210023, China.

[b]Shenzhen Research Institute of Nanjing University, Shenzhen 518063, China.

*Address correspondence to majing@nju.edu.cn, zhongjin@nju.edu.cn

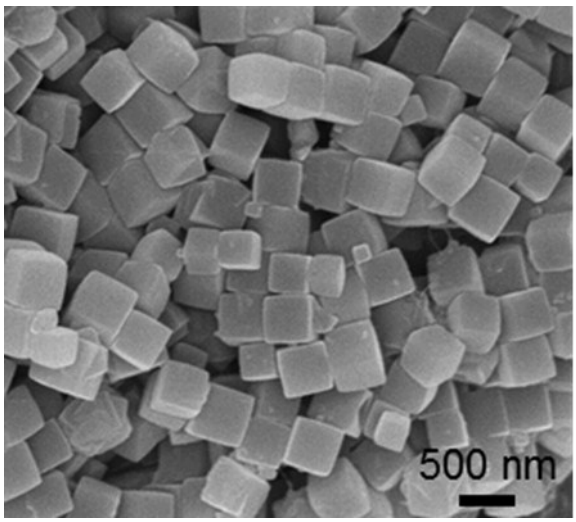

Figure S1. SEM image of ZIF-67 nanocubes.

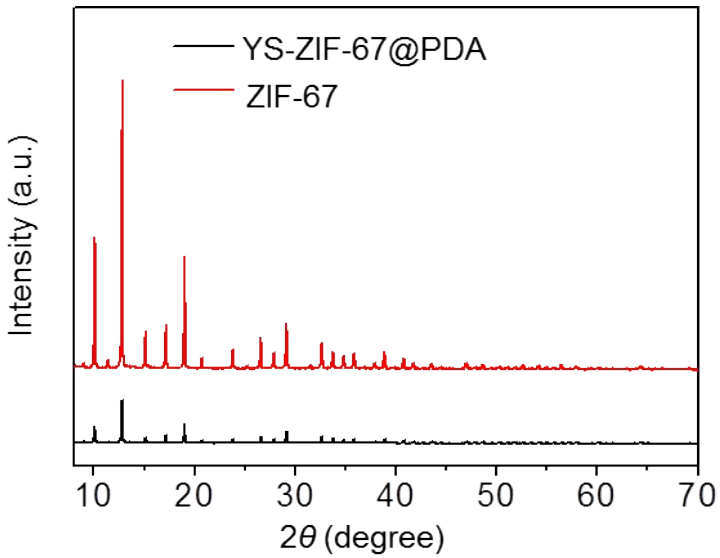

Figure S2. XRD patterns of ZIF-67 nanocubes and YS-ZIF-67@PDA nanocubes.

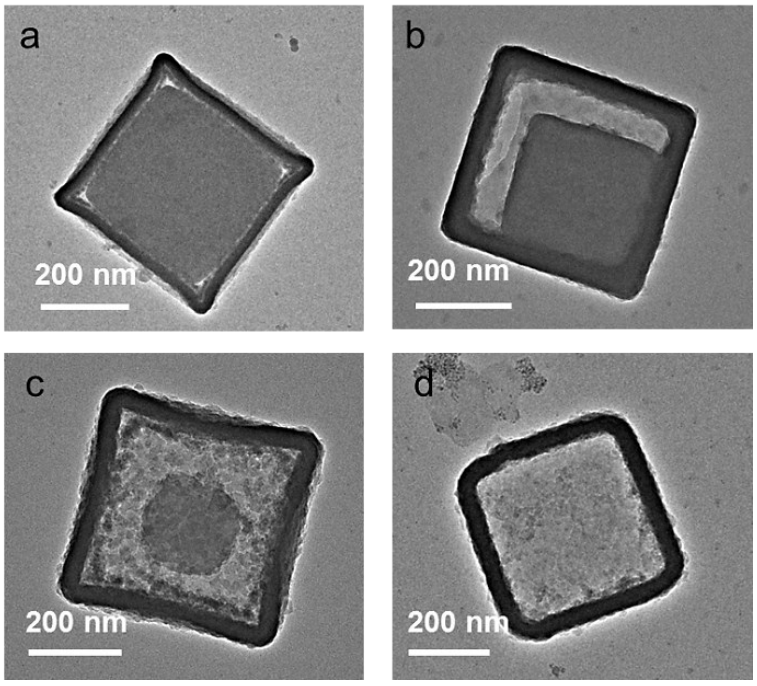

Figure S3. TEM images of ZIF-67@PDA nanoboxes obtained after the different reaction periods with dopamine: (a) 30 min, (b) 4 h, (c) 5 h, and (d) 7 h. After reacting for 7 h, the inner ZIF-67 yolks were completely dissolved, and only hollow PDA nanoboxes were remained, as shown in (d).

The dopamine molecules firstly captured the cobalt ions released from ZIF-67, leading to the disassembly of the nanostructure. Then, the released 2-methylimidazole (2-MIL) induced the polymerization of dopamine to form polydopamine (PDA) coating on the ZIF-67 surface. As the reaction goes by, the ZIF-67 cores were gradually dissolved due to the strong chelation between the catechol groups and Co ions, thus forming a hollow structure. Therefore, hollow carbon nanoboxes could be easily obtained by simply prolonging the reaction time.

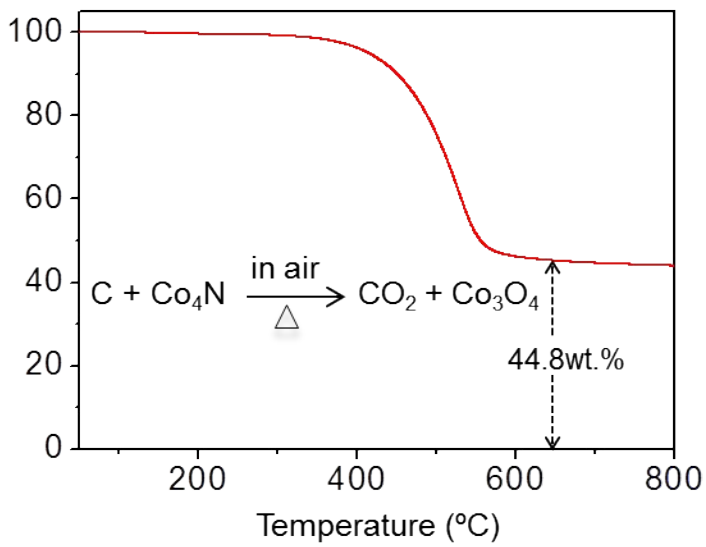

Figure S4. TGA curve of MYS-Co_4N@C nanoboxes in air with a heating rate of 10 $^oC\ min^{-1}$.

According to the reaction equation ($C + 3Co_4N \rightarrow CO_2 + 4Co_3O_4$), the mass ratio of Co_4N increased by 28.5% after the oxidation of Co_4N to Co_3O_4. The weight ratio of Co_4N (W_{Co4N}) was calculated as follows: $W_{Co4N} \times (100\% + 28.5\%) = 44.8\%$. Therefore, W_{Co4N} was calculated as 34.9 wt.%, and the weight ratio of carbon was estimated to be 65.1 wt.%.

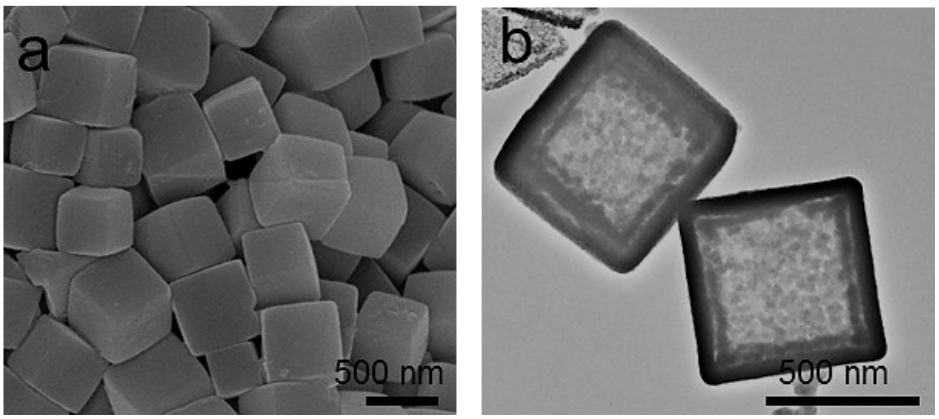

Figure S5. (a) SEM image of C-NBs, and (b) TEM image of C-NBs.

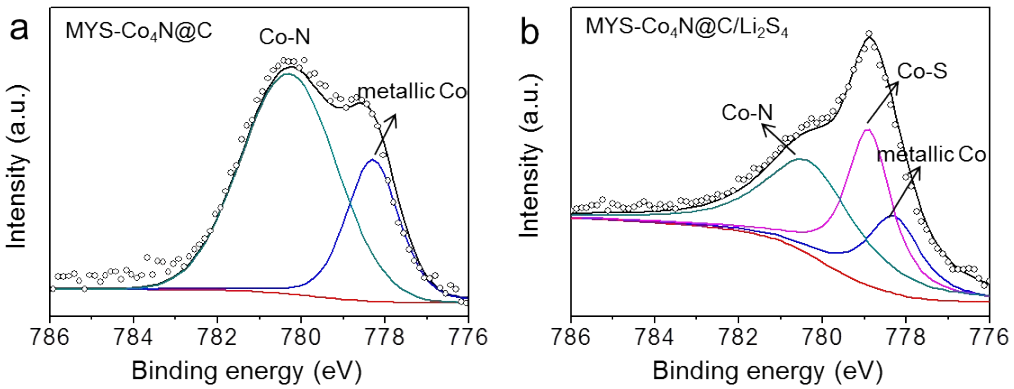

Figure S6. XPS spectra at Co $2p_{3/2}$ region of (a) MYS-Co_4N@C nanoboxes and (b) MYS-Co_4N@C/Li_2S_4 composite, respectively.

Table S1. Comparison of the cyclic performances of MYS-Co_4N@C/SeS_2 electrode in this work with other previously-reported Se_xS_y composite cathodes.

Ref.	SeS_2 host material	Areal SeS_2 loading (mg cm^{-2})	Cycle stability	Initial discharge capacity (mAh g^{-1})	Areal capacity (mAh cm^{-2})	Average capacity decay per cycle (%)
This work	**MYS-Co_4N@C/SeS_2**	**1.2**	**300**	**909 at 0.5 C**	**1.1**	**0.088**
		4.5	**100**	**850 at 0.1 C**	**3.8**	**0.13**
[S3]	HMC@TiN/SeS_2	5	80	880 at 0.05 C	4.4	0.20
		1	200	987 at 0.2 C	1.0	0.15
[S4]	SeS_2/MCA	1.5-2	250	816 at 0.45 C	1.6	0.25
[S5]	SeS_2/CMK-3@PDA	2.6-3	500	778 at 1.78 C	3.7	0.11
[S6]	CoS_2@LRC/SeS_2	2.3-3	400	868 at 0.45 C*	3.0	0.11
[S7]	Se_2S_5/MCM	0.5-0.8	100	1151 at 0.5 C*	0.9	0.31
[S8]	Se_2S_5/MPC	1-2	100	692 at 0.5 C*	3.1	0.38
[S9]	SeS_2/HMCNCs	1.2-1.5	100	986 at 0.18 C	1.45	0.16

* Se_2S_5 (1C = 1389 mA g^{-1})

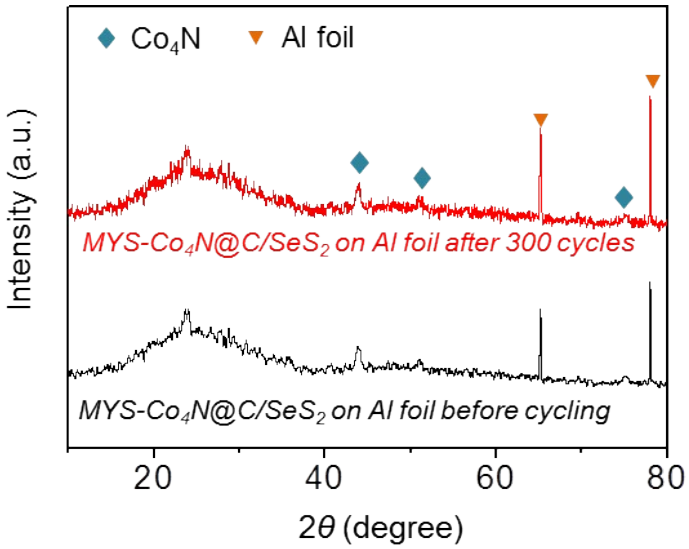

Figure S7. XRD patterns of MYS-Co_4N@C/SeS_2 electrode on Al foil before and after 300 cycles at 0.5 C.

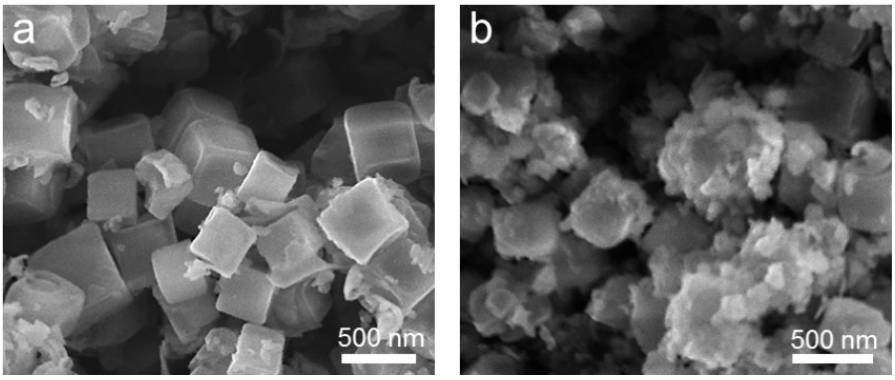

Figure S8. SEM images of (a) MYS-Co_4N@C/SeS_2 and (b) C-NBs/SeS_2 electrodes after 300 cycles at 0.5 C.

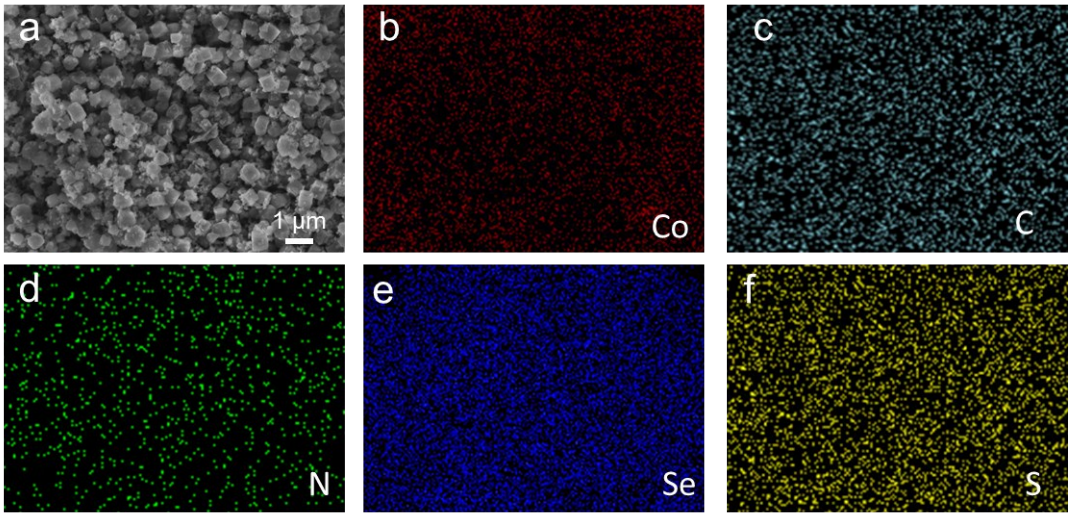

Figure S9. (a) SEM image and (b-f) corresponding elemental mappings of Co, C, N, Se, and S elements of MYS-Co_4N@C/SeS_2 electrode after 300 cycles at 0.5 C.

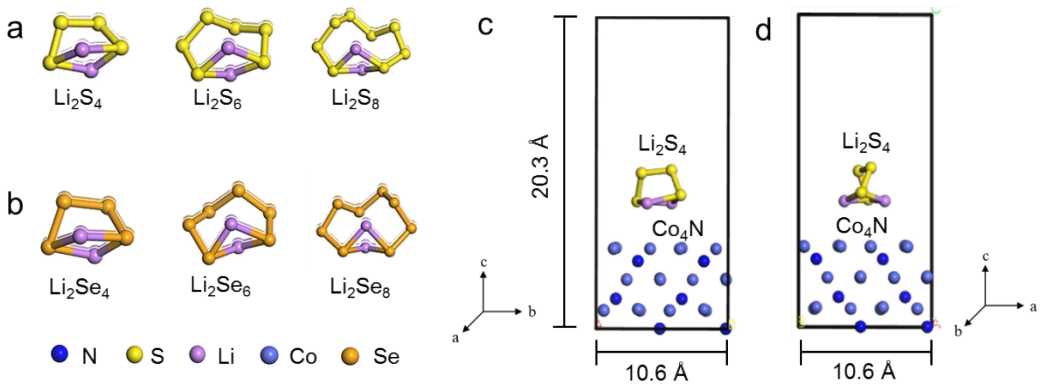

Figure S10. The optimized structures of (a) Li_2S_n and (b) Li_2Se_n (n = 4, 6, 8). The (c) front and (d) side views of the slab model of Li_2S_n or Li_2Se_n interacted with Co_4N. The cell size is set as 10.6 × 10.6 × 20.4 $Å^3$.

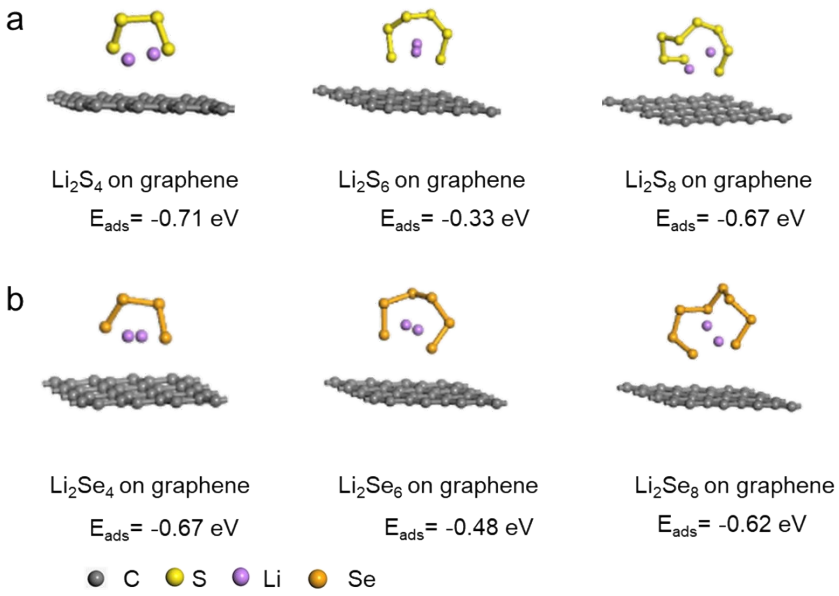

Figure S11. DFT calculation results of the adsorption geometric configurations and the calculated adsorption energies of (a) Li_2S_n and (b) Li_2Se_n (n = 4, 6 or 8) on graphene.

Table S2. DFT calculation Results of the energies of Li_2S_n and Li_2Se_n (n = 4, 6, 8) on the (111) planes of Co_4N.

	Li_2S_4@Co_4N	Li_2S_6@Co_4N	Li_2S_8@Co_4N	Li_2Se_4@Co_4N	Li_2Se_6@Co_4N	Li_2Se_8@Co_4N
E_s/eV	-1494.40	-2050.92	-2606.79	-1422.91	-1943.61	-2463.80
E_{sub}/eV	-53309.16	-53309.16	-53309.16	-53309.16	-53309.16	-53309.16
E_{s+sub}/eV	-54812.23	-55370.00	-55925.51	-54737.82	-55258.14	-55776.11
E_{ads}/eV	-8.68	-9.93	-9.56	-5.75	-5.37	-3.16

Table S3. DFT calculation results of the adsorption energies of Li_2S_n and Li_2Se_n (n = 4, 6 or 8) on graphene.

	Li_2S_4 @graphene	Li_2S_6 @graphene	Li_2S_8 @graphene	Li_2Se_4 @graphene	Li_2Se_6 @graphene	Li_2Se_8 @graphene
E_s/eV	-1494.40	-2050.92	-2606.79	-1422.91	-1943.61	-2463.8
E_{sub}/eV	-4965.22	-4965.22	-4965.22	-4965.22	-4965.22	-4965.22
E_{s+sub}/eV	-6460.34	-7016.48	-7572.68	-6388.81	-6909.31	-7429.64
E_{ads}/eV	-0.71	-0.33	-0.67	-0.67	-0.48	-0.62

Computational method. Density functional theory (DFT) calculations were carried out to study the possible adsorption behaviors of Li_2S_n/Se_n (n=4,6,8) on Co_4N slab. A slab model of Co_4N with the cell size of 10.6 × 10.6 × 20.4 $Å^3$ (as shown in **Figure S10**) was built. The vacuum thickness is set to 15 Å, in order to avoid the interactions between successive slabs. And simultaneously at the same level of calculation, a model Li_2S_n/Se_n@ graphene, of which the cell size is 9.8 × 9.8 × 20.4 $Å^3$, was built as a comparison. The stable adsorption structures and the final energies were obtained by using Cambridge Sequential Total Energy Package (CASTEP) simulation package[S1,2] in the Materials Studio 7.0. Generalized gradient approximation (GGA) in the form of Perdew–Burke–Ernzerhof (PBE) functional was employed for the DFT exchange correlation energy, and ultrasoft pseudo-potentials were used for the core electrons. Grimme's method was added to the GGA energy to describe the long-range-

interactions[S1].

The adsorption energy E_{ads} of Li_2S_n/Se_n (n=4,6,8) is calculated by:

$$E_{ads} = E_{s+sub} - E_s - E_{sub} \quad (1)$$

where E_{s+sub} and E_{sub} are the total energies of the surface with and without the Li_2S_n/Se_n (n=4,6,8) adsorbate, respectively, and E_s is the energy of a Li_2S_n/Se_n (n=4,6,8) molecule in vacuum atmosphere. A plane-wave basis set with an energy cutoff energy of 450 eV was assigned and the self-consistent field (SCF) tolerance was 2.0×10^{-6} eV/atom. The convergence criteria of geometry optimizations were set to be 2.0×10^{-5} eV/atom for energy, 5.0×10^{-2} eV/Å for the gradient, and 2×10^{-3} Å for the displacement, respectively.

Theoretical calculations, as shown in **Table S2**, hint that these molecules tend to be well trapped when Co_4N presents, inhibiting the shuttle issue of polysulfieds and polyselenides, while they seem to be not well trapped on graphene (Table S3).

Reference

[S1] Z. Chen, Y. Song, J. Cai, X. Zheng, D. Han, Y. Wu, Y. Zang, S. Niu, Y. Liu, J. Zhu, X. Liu, G. Wang, *Angew. Chem. Int. Ed.* **2018**, *57*, 5076.

[S2] Z. H. Li, Q. He, X. Xu, Y. Zhao, X. W. Liu, C. Zhou, D. Ai, L. X. Xia, L. Q. Mai, *Adv. Mater.* **2018**, *30*, 1804089.